FOUTH EROPEAN ROTORCRAFT AND POWERED LIFT AIRCRAFT FORUM

Paper No 8

AN INVESTIGATION OF THE INFLUENCE OF FUSELAGE FLOW FIELD ON ROTOR LOADS, AND THE EFFECTS OF VEHICLE CONFIGURATION

P G Wilby, C Young and J Grant
Royal Aircraft Establishment
England

September 13 - 15, 1978
STRESA, ITALY

Associazione Italiana di Aeronautica ed Astronautica
Associazione Industrie Aerospaziali

AN INVESTIGATION OF THE INFLUENCE OF FUSELAGE FLOW FIELD ON ROTOR LOADS, AND THE EFFECTS OF VEHICLE CONFIGURATION

P G Wilby C Young and J Grant

Royal Aircraft Establishment

1 Introduction

The idea that the flow disturbances due to the fuselage of helicopter can affect the loads and motion experienced by the rotor is not a new one. An early study of the influence of the fuselage of a Wessex helicopter on the flapping motion of the blades[1] concluded that the effect was not significant. Our present interest in the topic started a few years ago when predicted blade loadings for an S58 helicopter were being compared with flight experiments[2]. It was found that an appreciable difference between theory and measurement existed over the inner part of the blade for a narrow band of azimuth angle centred on 180°. This difference could be accounted for if a modification to blade incidence was made in the prediction method that was compatible with the upwash provided by a simple representation of the fuselage. At about the same time, in some flight experiments at the RAE on a Wessex helicopter,[3] roughness was applied to the blade leading-edge to lower the stalling incidence. This resulted in blade stall being provoked in the region of 60% rotor radius at 180° azimuth in forward flight, indicating that blade incidence can be quite high in this region of the rotor disc. More recent RAE flight experiments on a Puma helicopter[4] have indicated a perturbation in blade incidence as the blade passes through 180° azimuth, which may be due to fuselage flow effects. The influence of the fuselage has attracted the attention of other researchers[5] who conclude that it can cause a large increase in blade incidence around 180° azimuth, and that this must be taken into account when calculating blade loading.

As the fuselage of the modern helicopter tends to extend further and further forwards, relative to the rotor hub, any disturbance it causes is moved further outboard along the blade, to a region of higher dynamic pressure, and its effect is therefore likely to be accentuated. The current trend towards more compact helicopter designs, involving a lowering of the rotor and a decrease of the clearance between the fuselage and rotor, will further increase the influence of the fuselage on rotor loads. A more thorough study of fuselage flow effects is clearly needed and some of the results of this study are presented in this paper.

The questions to be answered are, what is the magnitude of the change in blade loading due to the fuselage flow, what are the contributing factors and do the resulting loads lead to a significant increase in rotor vibratory loading.

2 Fuselage Flow Field Calculations

The first step in the investigation was to develop a suitable method for predicting the flow field, due to a fuselage, in the plane of the rotor. An existing panel method, used for wing-body calculations, was adapted for this purpose and modified to give velocity components normal to a disc at any specified position parallel to the body axis. One problem with such a calculation is that a large number of fuselage ordinates have to be generated. For simplicity, it was decided that the cross section of a fuselage could be

represented in the way shown in Figure 1. The sides, top and bottom have flat surfaces and the corners are elliptic, with double symmetry assumed. Only four parameters (D, W, d and w) are needed to define any shape from a circle (D = W; w = d = o) or an ellipse (D $\neq$ W; w = d = o) to a rectangle (D = d, W = w). In between these extremes lies a whole range of shapes with flat sides and rounded corners. By varying these parameters along the length of the fuselage, typical helicopter shapes can be described, provided a further parameter, the height, h, of the mean line above the datum, is prescribed. A simple general expression can be derived to give the co-ordinates of the cross section for any value of the angle θ (defined in Figure 1). Then, by specifying the five parameters shown in Figure 1, a complete set of fuselage co-ordinates can be calculated for a set of values of θ and x.

Calculations have been made for fuselage shapes representing the Puma and Lynx helicopters, being examples of modern designs. The vertical component of velocity in the plane of each rotor is given in Figure 2 for 180° azimuth. As might be expected, the maximum value is found near the front of the cabin roof, following the steeply inclined line of the windshield. The way in which upwash decays on either side of 180° azimuth is shown in Figure 3, where we see that at 40% rotor radius the upwash has fallen to half its maximum value over 25° to 30° azimuth.

Having obtained the upwash over the rotor disc it was then introduced into a program for calculating the blade loading and rotor performance. An iterative calculation is used in which the wake is represented by a series of vortex rings. The process converges onto a different solution depending on whether or not the fuselage upwash is included. The upwash is introduced as a modification to the rotor downwash field prior to the calculation of blade loading. Figure 4 gives the calculated blade incidence distribution at 180° azimuth for a Lynx helicopter at 140 knots and shows the effect of the fuselage flow. The lower part of Figure 4 gives the change in incidence due to the fuselage upwash, together with the value that might be inferred on the basis of upwash velocity and blade velocity alone. For this particular case, the maximum change in blade incidence is 8.5° at about 30% rotor radius, giving a total incidence there of 13°. It should be noted here that the blade incidence still lies within the boundary (see Figure 4) set by the stall angle for the blade section (RAE 9615) in steady conditions[6].

Although a fuselage incidence of zero has been taken in these calculations, the flow field program will run for any specified fuselage incidence (but of course, for potential flow). The effect of a 4° nose-down attitude on the simple evaluation of blade incidence is shown in Figure 5, where an additional 1.5° in blade incidence is found at 30% rotor radius. As the Lynx fuselage attitude at 140 knots is only 1° nose-down[7], the effect on blade incidence is negligible and any further results presented here are for zero fuselage incidence. A further factor that should be considered is that, in the calculation, the rotor blade is assumed to lie in a plane that is parallel to the fuselage datum. Strictly, the affect of coning angle and disc tilt should be taken into account. To assess the importance of the simplification, fuselage upwash is presented in Figure 6 at two different heights above the fuselage. There is little change in upwash with height near the blade tip, but an appreciable change over the inboard region. Thus, provided the plane in which upwash is calculated represents the height of the inboard part of the rotor blade above the fuselage, then errors due to the simplified approach will be small.

The theoretical results presented so far have been obtained with what we refer to as the performance program. This assumes that the blades themselves are rigid except in torsion. For the investigation of blade loads we need a full representation of the blade dynamic characteristics and this requires the coupled modes program in which flap, lag and torsion modes are introduced. Both these programs are based on ones developed by Westland Helicopters and are referred to in the remainder of this paper.

3 The Effect of Fuselage Upwash on Rotor Loads for the Lynx Helicopter

Although the fuselage upwash increases incidence considerably over the inner part of the blade at 180° azimuth for the Lynx helicopter (Figure 4), the dynamic pressure over this region of the blade is low and the effect on blade lift distributions is fairly small, as is seen in Figure 7. In Figure 8 (a) the azimuthal variation of the blade lift coefficient is given and the effect of the fuselage upwash is seen to cause only a small perturbation on the rotor alone value. The magnitude of the amplitude of the variation is unaltered. Figure 8 (b) gives the azimuthal variation of blade torque, due to aerodynamic drag, and again the fuselage flow causes only a small perturbation. The decrease in blade torque in the region of 180° azimuth arises from the reduction in induced drag due to the upwash of the fuselage.

The coupled modes program was used to calculate the response of the rotor to these small changes in aerodynamic loading at 140 knots, with 8 modes (4 flapwise, 3 lagwise and 1 torsion) being represented. The predicted changes in blade bending moments at 13.5% rotor radius are shown in Figure 9. The change in flapwise moment has a strong 3 cycles per revolution content, and the change in lagwise moment has a strong 4 cycles per revolution content. These observations combined with the interference diagram for the Lynx rotor (Figure 10) suggest that the 2nd flap and 2nd lag modes are being excited, which is to be expected even though their natural frequencies are reasonably well clear of resonance. It could be argued that these modes are likely to be excited because their shapes are similar to the form of the spanwise distribution of the forcing loads.

It should be pointed out here that the peak to peak variation of flapwise bending moment is not altered by the presence of the fuselage, but the peak to peak lagwise moment is increased by about 30%. It can then be noted that the agreement between predicted and measured amplitude of the flapwise moment was found to be very good by Westland Helicopters[7], whereas the amplitude of the lagwise moment was found to be considerably larger than predicted. The difference in influence on the two moment variations follows from the fact that peaks in the lagwise moment perturbation coincide with peaks in the lagwise moment variation for the rotor alone. This does not happen with the flapwise moments.

Hub forces and moments are important from the vibration point of view, and Figure 11 gives the predicted azimuthal variation of pitching moment, axial force and in-plane force for rotor alone and with fuselage effects. The amplitude of the fore and aft in-plane force is doubled by the presence of the fuselage whereas the pitching moment and axial force amplitudes are slightly decreased. In Ref 8 the agreement between predicted and measured pitching-moments and axial force was quite good whilst the measured in-plane force had double the predicted amplitude at 140 knots. Fuselage effects again appear to offer an explanation for some of the discrepancy.

The results of these calculations can be summarised by saying that the upwash due to the fuselage of a Lynx helicopter appears to increase the lagwise bending moment by about 30%, and doubles the amplitude of the fore and aft in-plane force. However, this is not to suggest that the rotor clearance is too small, as Figure 6 shows that even if it was increased by 30% the fuselage effects would be reduced by only 20%.

4 Wind Tunnel Model Tests and Comparison with Theory

In order to check the theoretical methods that were being used to calculate the effect of the fuselage, a model rotor test programme was devised for the 24 ft wind tunnel at the RAE[9]. A fuselage model was placed below an existing model rotor[10] and measurements of bending-moments made on the flap and lag flexures of one particular blade (the 3-bladed rotor is non-articulated in flap and lag). Tests were carried out for two fuselage shapes (Figure 12), and a range of rotor height, rotor speed, advance ratio and thrust.

The experimental results are being compared with theoretical predictions given by the coupled modes rotor loads program. Five blade modes have been included in the calculations, three flap and two lag, which are all the modes with a frequency of less than 150 hz (see Figure 13).

Some of the comparisons between theory and experiment are presented in Figures 14 to 16. Each figure shows the measured and calculated change in the flatwise bending moment on the flap flexure at 9.4% rotor radius, due to the addition of the fuselage. The configuration for all these cases is as shown in Figure 12 (a) with the lowest of the three rotor positions.

The bending moment increment for a rotor speed of 400 rev/min, collective pitch of 8.7° and advance ratio of 0.3, is virtually undamped at $6\,\Omega$ which is coincident with the second flap mode frequency (see Figure 13). The calculated oscillation is more damped than the measured one on both the retreating and advancing sides of the disc, but is again essentially of $6\,\Omega$ frequency. At 500 rev/min (Figure 15) we have basically a $5\,\Omega$ oscillation for both experimental and theoretical results but with different degrees of damping. Again, we note that 5Ω is very close to the 2nd flap mode frequency. For this case, the measurements show a virtually undamped oscillation on the retreating side of the disc which is rapidly damped in the advancing sector, while theory predicts a progressive damping all round the disc. With a further increase of rotor speed to 600 rev/min, the measurements show a mildly damped oscillation with theory predicting slightly greater damping. At this rotor speed the oscillation is attempting to achieve a frequency of about $4.5\,\Omega$. Once again, it is the 2nd flap mode that is being excited even though the 3rd flap mode frequency is closer to resonance.

In an attempt to reduce the differences between measured and predicted results, the structural damping of the modes in the calculation was changed but this had no significant effect. It is possible that the differences in damping are of aerodynamic origin and may be related to differences in fuselage flow field at the rear of the rotor disc, where inviscid flow calculations are not expected to be accurate.

For the experimental results, it was found that the effect of the fuselage on the magnitude of the peak to peak flatwise bending moments depended upon the rotor speed. As we have already seen, the frequency of the bending moment perturbation varies with rotor speed, thus the phasing between

perturbation peaks and rotor-alone peaks will vary with rotor speed. At 400 rev/min we have a coincidence of peak values (Figure 17), giving an increase in peak to peak variation, but at 600 rev/min this does not occur. We thus have the result that although the perturbations at 600 rev/min are larger, in proportion to the undisturbed amplitude, than at 400 rev/min, they actually lead to a reduction in peak to peak load as apposed to an increase at 400 rev/min. At the time of writing this paper, the experimental lag bending moments had not been analysed. However, on the basis of the flatwise moments comparisons, one can conclude that the theory predicts the effects of the fuselage reasonably well but with an underestimate of the amplitude of the oscillatory perturbation.

5 Features that can Increase Blade Incidence at 180° Azimuth

The calculations so far presented for the Lynx helicopter indicate that the blade is well below stalling incidence over the forward part of the rotor disc at 140 knots at sea level. The possibility of large fluctuations in control loads caused by blade stall does not appear to be a problem with this helicopter. Flight tests at the RAE on a Puma helicopter[4], which provides a similar fuselage upwash field to that of the Lynx (see Figure 2), have also indicated an absence of blade stall at the front of the disc. In these tests, pressure was measured at the leading and trailing-edges of a blade at 17 spanwise stations over the outer half of the blade. The leading-edge pressures give an indication of blade incidence, and show a disturbance centred on 180° azimuth in Figure 18. There was no sign of trailing-edge pressure divergence, which is used as an indication of flow separation, even at a speed of 140 knots at 2500 m altitude. However, this does not rule out the possiblity of blade stall at 180° azimuth for other helicopter configurations and flight conditions. Wake distortion, increased forward speed, increased blade twist and different fuselage shapes can all provide increases in blade incidence and make stall more likely. The importance of these factors will now be considered, using the performance program.

5.1 Wake distortion

The wake model used in the calculation consists of an array of vortex rings, in planes normal to the rotor shaft but displaced longitudinally and vertically according to forward flight and downwash velocities. The vertical displacement Δz, between each vortex ring is given by

$$\frac{\Delta z}{R} = \frac{2\pi\bar{v}}{b\Omega R}$$

where $\bar{v}$ is the mean downwash velocity and b the number of blades. In the real case, with the influence of the fuselage, the distribution of downwash velocity over the rotor disc is very uneven and the vortex generated by the blade tip at 180° azimuth is likely to stay very close to the rotor disc as it is transported rearwards. To evaluate the possible effects of such a feature of the vortex wake, the first vortex ring in the wake model has been distorted by taking

$$\frac{\Delta z}{R} = (1 + \mu k \sin^2\tfrac{1}{2}\psi \cos^5\psi) \frac{2\pi\bar{v}}{b\Omega R}$$

where k can be specified as desired. Advance ratio μ is included in the distortion term because the fuselage upwash, and hence the vortex displacement, is directly proportional to forward speed. The distortion term is chosen to give a variation with azimuth that is similar to the form of the variation of fuselage upwash, as seen in Figure 19. Using this expression, the vortex distortion is effectively zero outside the range $120^\circ < \psi < 240^\circ$.

With this modified form of the vortex ring wake model, the aerodynamic loading on a Lynx rotor at 140 knots has been calculated, and the blade incidence distributions at 180° azimuth are shown in Figure 20 for k = o and 2.5. With the resulting close proximity of the vortex from the previous blade, the predicted blade incidence at mid span is increased by about 5°, giving a value of incidence slightly in excess of the static stall value. It is clearly important to have an accurate representation of the effect of the fuselage flow on the vortex wake if a reliable prediction of blade incidence is to be attained.

5.2 Blade twist and forward speed effects

An increase of blade twist naturally tends to increase blade incidence over the inner part of the disc. Figure 21 shows the predicted changes in blade incidence at 180° azimuth if the twist of the Lynx rotor were increased from 8° to 12° and 16°. Doubling the twist would increase incidence by 2.5° over the inner part of the blade at a forward speed of 140 knots.

Also shown in Figure 21 is the increase in blade incidence resulting from an increase of forward speed from 140 to 160 knots. This also amounts to 2.5° over the inner part of the blade at 180° azimuth. Although the blade incidence for the Lynx would then slightly exceed the static stall incidence for the blade section over a small extent of blade, no serious stall effects would be anticipated.

5.3 Fuselage shape

The fuselage shape and its position relative to the rotor disc have a direct influence on upwash in the plane of the rotor and hence on blade incidence. To give some indication of the sensitivity of upwash to fuselage configuration, the predicted upwash at 180° azimuth is given in Figure 22 for several variations of fuselage shape. The plane in which upwash is calculated is shown in Figure 22. Summarizing the results, the steepness of the cabin windshield line has little effect on upwash, but the form of fairings on top of the fuselage has a considerable effect. For fuselage shape 5 in particular there is a considerable reduction in upwash over the inner blade if the rotor is raised from position 'a' to position 'b' as shown in Figure 23.

The effect of varying the forward extension of the fuselage nose relative to the hub can be assessed simply by imposing a transverse displacement on the upwash distribution.

A further possible change in fuselage shape is a change in width, and Figure 24 gives the upwash distribution for a fuselage of half the width but with the same sideways profile as shape 1. A considerable reduction in upwash is found for the slim fuselage.

5.4 A combination of features that will produce blade stall at 180° azimuth

On the basis of the results obtained so far, a configuration was selected that is likely to produce blade stall at 180° azimuth. Fuselage shape 5 was chosen with the rotor in close proximity, as shown in Figure 22. A rotor of the same dimension as the Lynx rotor but with 16° twist (in place of this normal 8°) was taken, and the tip vortex from the previous blade was distorted in the way outlined in Section 5.1, taking $k = 2.5$. The blade incidence at 180° azimuth for a speed of 140 knots as given by the rotor performance program is plotted in Figure 25. Incidence is seen to be well in excess of the static stall incidence over the inner part of the blade. The performance program includes a representation of dynamic stall as developed by Westland Helicopters[11], and the predicted azimuthal variation of root pitching moment is shown in Figure 26, compared with the value for rotor alone. In the top part of Figure 26 are the corresponding variations of root pitching moment for the standard Lynx rotor. It is seen that the blade does in fact stall at 180° azimuth for the selected configuration, producing a considerable oscillatory increment to the pitching moment. This will of course be reflected in an oscillation superimposed on the control loads. Stall will also produce considerable variations in blade drag and an extra aerodynamic forcing for additional oscillatory lag bending moments and in-plane hub forces. In such a case as this, there would be considerable benefits in raising the height of the rotor.

6 Conclusions

Although the study of fuselage effects on rotor loads is not complete and is certainly not exhaustive, various points have emerged that are worth emphasising.

a. Calculations indicate that fuselage upwash can provide a perturbation to aerodynamic forces which lead to a significant blade and hub response in a form depending upon the stiffnesses of the rotor blades, even when blade stall is not precipitated. For the Lynx helicopter the effect shows up as an increase in blade lagwise bending moment and in-plane hub force. In such a case, where blade stall is not present, raising the rotor height would not have a large effect on the loads generated.

b. Results from wind tunnel tests on a model rotor have shown that the method for predicting the effect of fuselage flow on rotor loads is reasonably accurate, with perhaps a slight underestimate of the true magnitude.

c. The theoretical study of the factors that tend to increase blade incidence at 180° azimuth shows that it is possible with some helicopter configurations to produce stall over the inner part of the blade in the forward sector of the disc. Stall can be sufficiently severe to cause large oscillations in blade root torsional load and a much increased variation of blade drag. The latter is likely to amplify further the blade bending moments.

d. The calculations show the importance of developing an accurate representation of the way in which fuselage upwash distorts the vortex wake when modelling the wake for the calculation of rotor downwash.

e. A general conclusion is that the influence of fuselage upwash is important and must be taken into account when calculating blade and hub loads.

References

1 M A P Willmer. Effect of flow curvature due to the fuselage on theflapping motion of a helicopter rotor. RAE Tech Note Naval 61 (1963).

2 J Scheiman. A tabulation of helicopter rotor blade differential pressures, stresses, and motions as measured in flight. NASA TM X-952 (1964).

3 M J Riley. A flight investigation of the spanwise lift requirements of a helicopter rotor blade by measurement of the control loads arising from locally applied roughness. ARC R&M 3812.

4 P Brotherhood, M J Riley. Flight experiments on aerodynamic features affecting helicopter blade design. Vertica, Vol 2 pp 27-42 (1978).

5 A J Landgrebe, R C Moffitt, D R Clark. Aerodynamic technology for advanced rotorcraft. Journal of the American Helicopter Society, Vol 22 No 3 July 1977.

6 N Gregory, P G Wilby. NPL 9615 and NACA 0012; a comparison of aerodynamic data. ARC CP No 1261 (1973).

7 K T Mckenzie, D A S Howell. The prediction of loading actions on high speed semi-rigid rotor helicopters. AGARD CP No 122 (1973).

8 V A B Rogers. The design of the WG 13. The Aeronautical Journal, January 1974.

9 R J Marshall. Wind tunnel tests on the influence of rotor-to-fuselage proximity on helicopter blade loads. RAE Technical Report to be published.

10 A Anscombe, A P Cox, R J Marshall. Wind tunnel testing of model rotors at RAE Farnborough. Proceedings of the 2nd European Rotorcraft and Powered Lift Forum, Buckeburg, 1976.

11 T S Beddoes. A synthesis of unsteady aerodynamic effects including stall hysteresis. Proceedings of the 1st European Rotorcraft and Powered Lift Forum, Southampton, 1975.

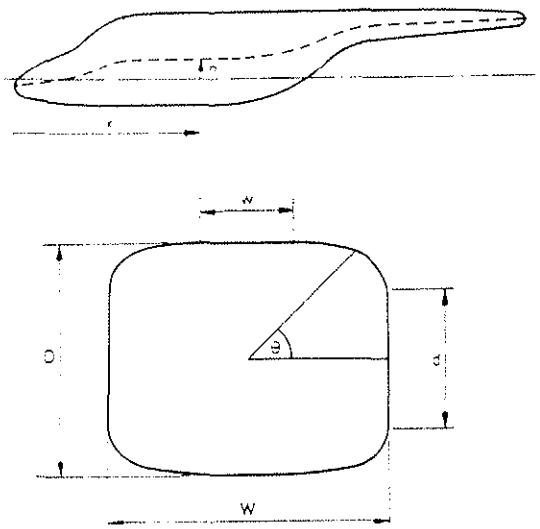

Fig 1 Parameters to be specified for the calculation of fuselage co-ordinates

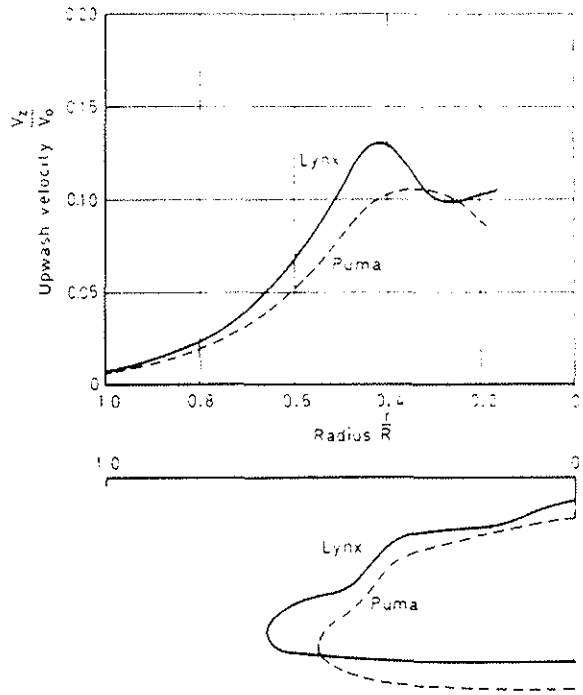

Fig 2 Calculated upwash in plane of rotor at 180° azimuth for Lynx and Puma fuselages

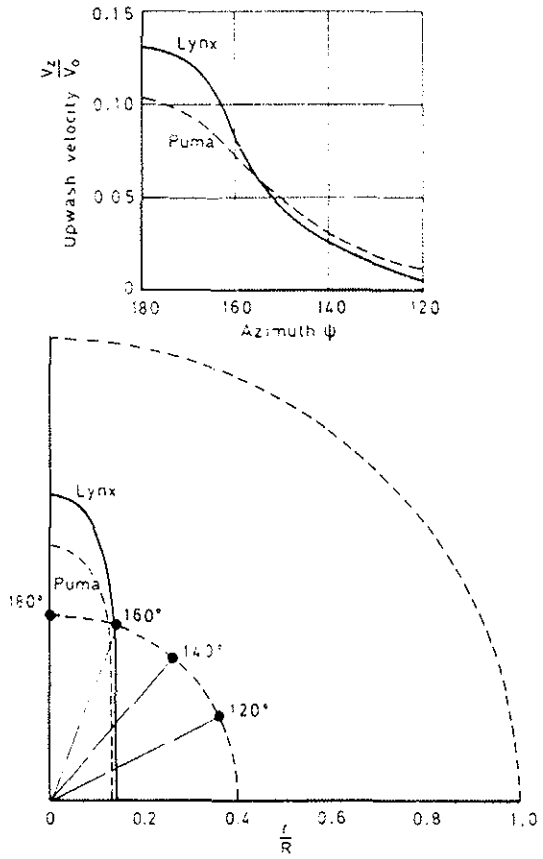

Fig 3 Predicted azimuthal variation of fuselage upwash in plane of rotor at 40% radius for Lynx and Puma helicopters

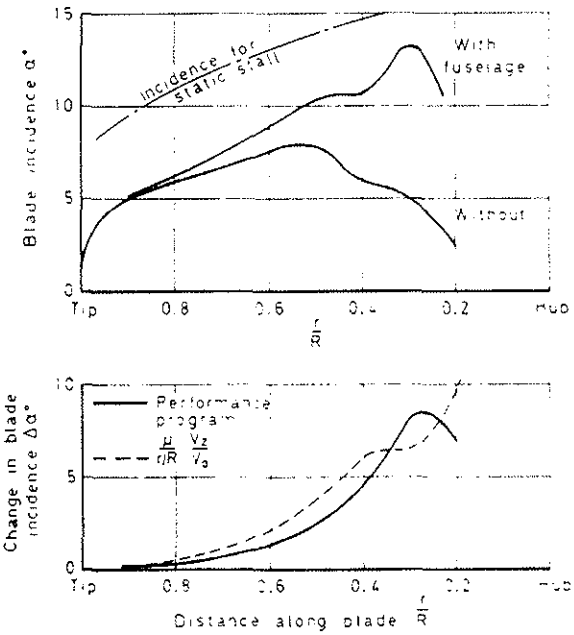

Fig 4 Predicted effect of fuselage upwash on blade incidence at 180° azimuth for Lynx helicopter at 140 knots

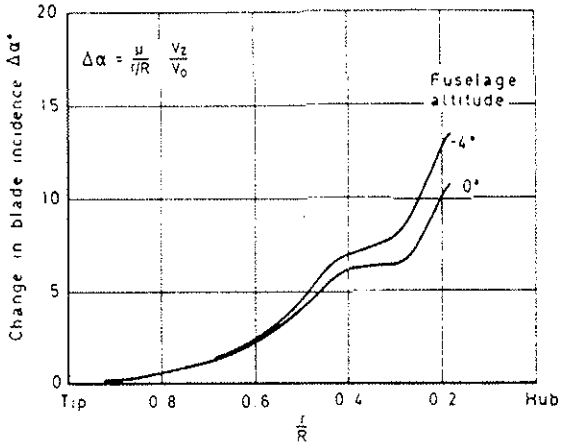

Fig 5 Predicted effect of fuselage attitude on change of blade incidence due to fuselage upwash at 180° azimuth

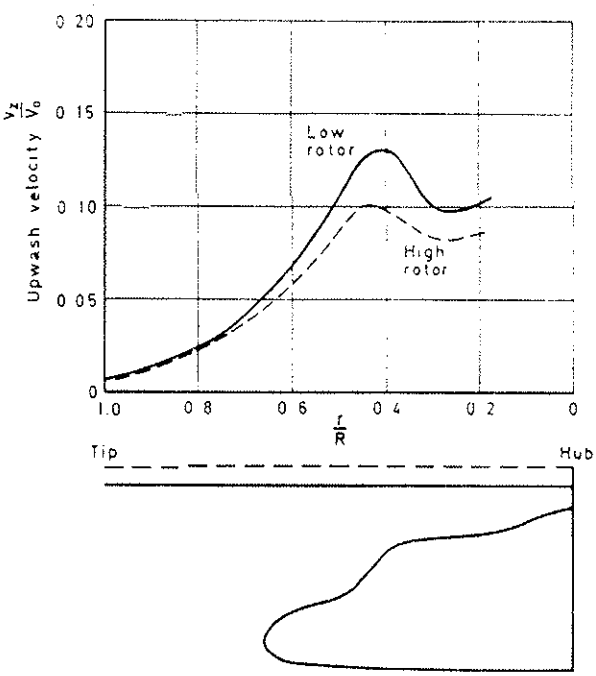

Fig 6 Predicted variation of fuselage upwash with height above the fuselage at 180° azimuth

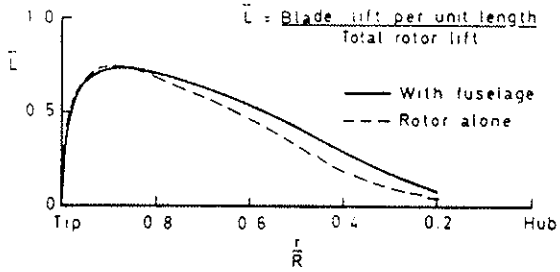

Fig 7 Predicted effect of fuselage upwash on blade loading at 180° azimuth for Lynx rotor at 140 knots

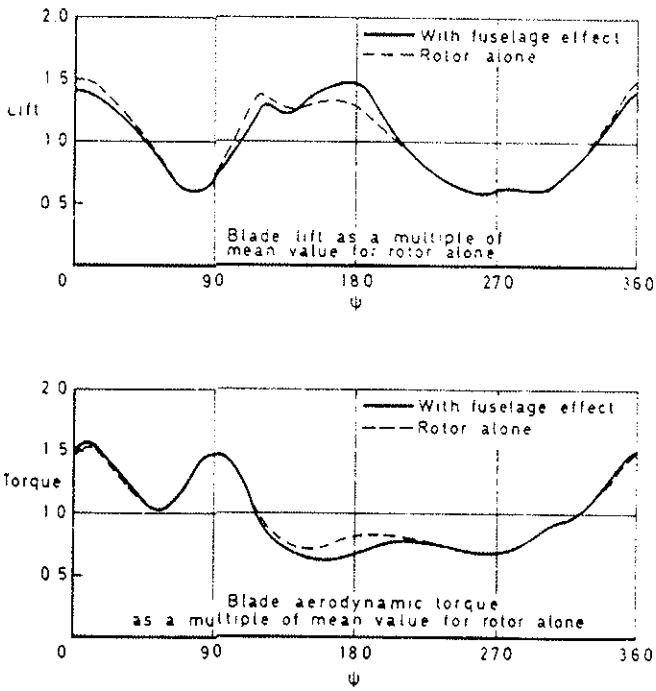

Fig 8 Predicted effect of fuselage upwash on azimuthal variation of blade lift and torque for Lynx helicopter at 140 knots

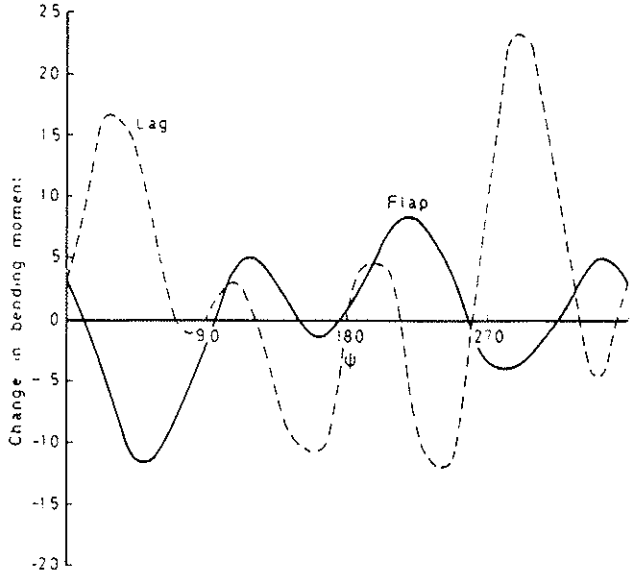

Fig 9 Predicted change in flapwise and lagwise bending moments for Lynx rotor due to fuselage flow, taken as a percentage of peak to peak variation for rotor alone

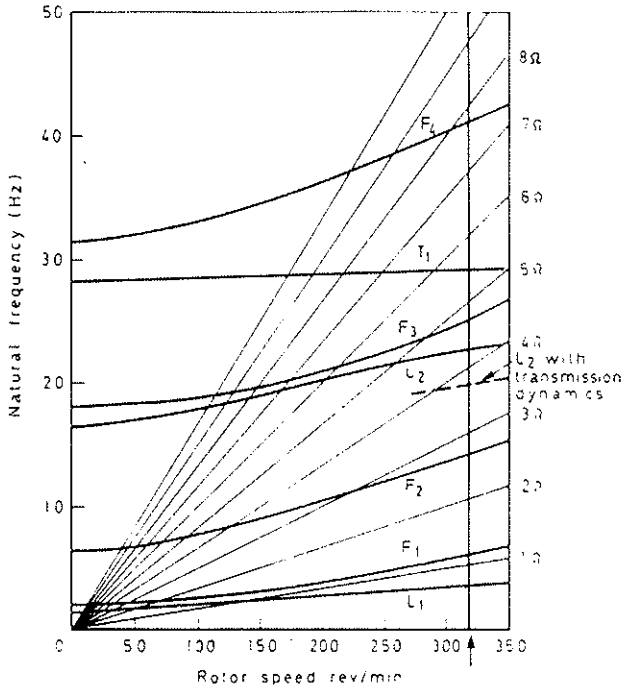

Fig 10 Interference diagram for Lynx rotor

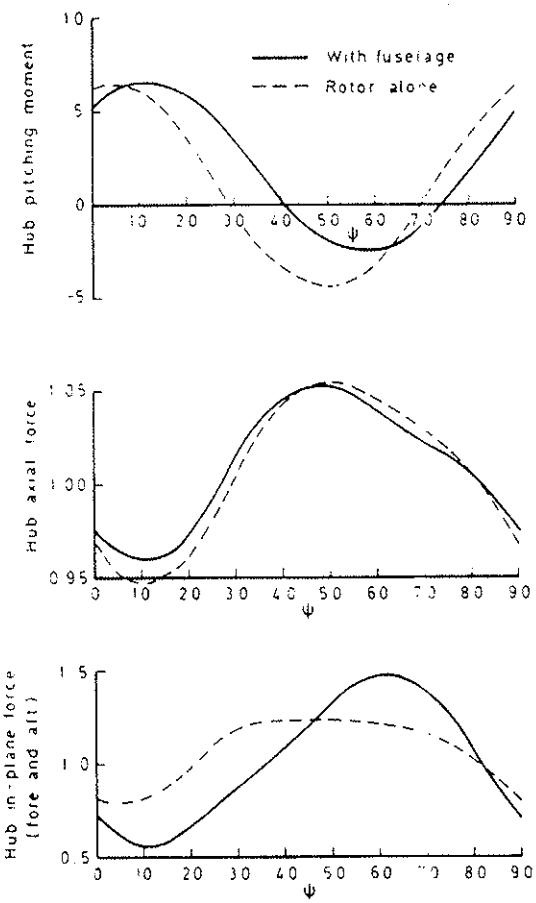

Fig 11 Predicted hub moment and forces with and without fuselage flow effects, as a multiple of mean value for rotor alone for Lynx

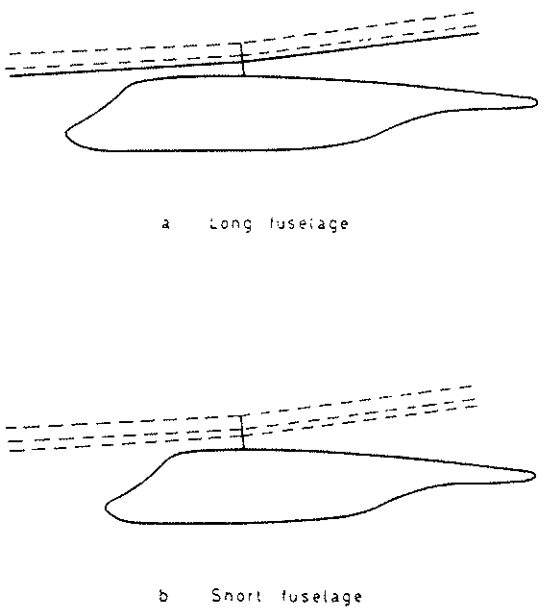

Fig 12a&b Model helicopter configurations

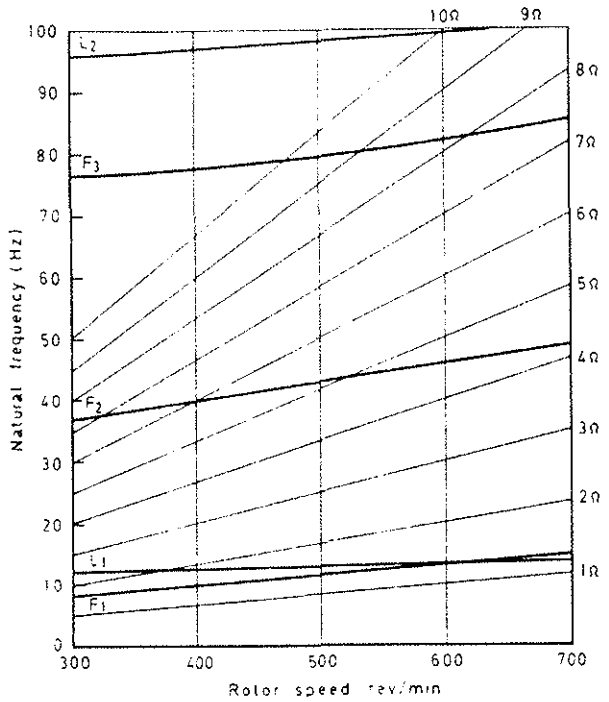

Fig 13 Interference diagram for RAE model rotor

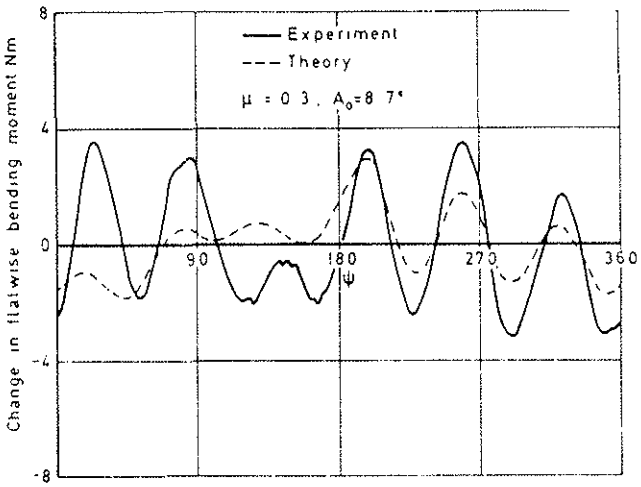

Fig 14 Predicted and measured effect of fuselage on model blade flatwise bending moment at 400 rev/min

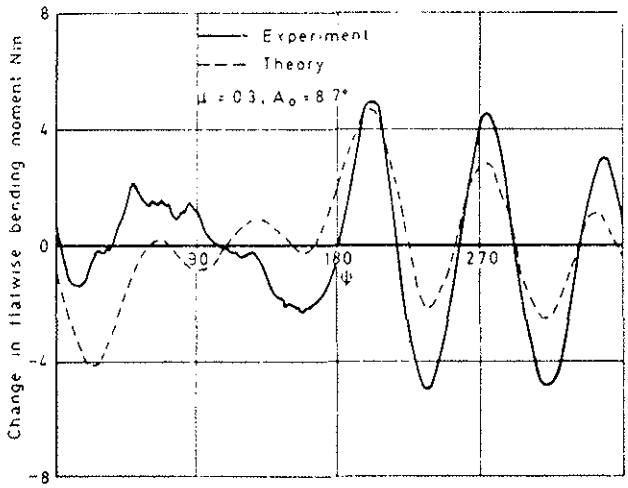

Fig 15 Predicted and measured effect of fuselage on model blade flatwise bending moment at 500 rev/min

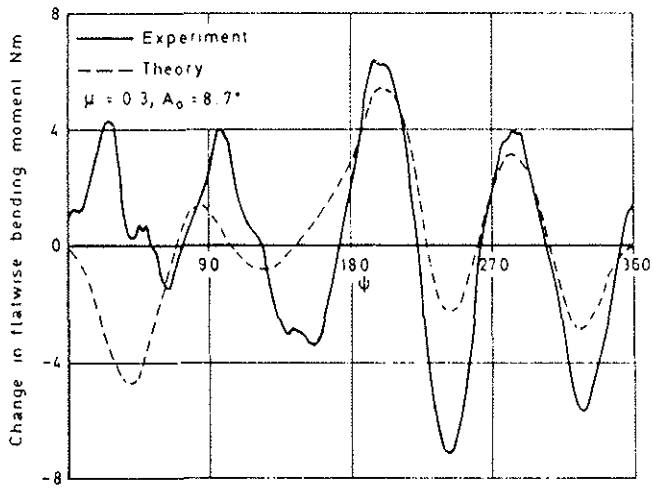

Fig 16 Predicted and measured effect of fuselage on model blade flatwise bending moment at 600 rev/min

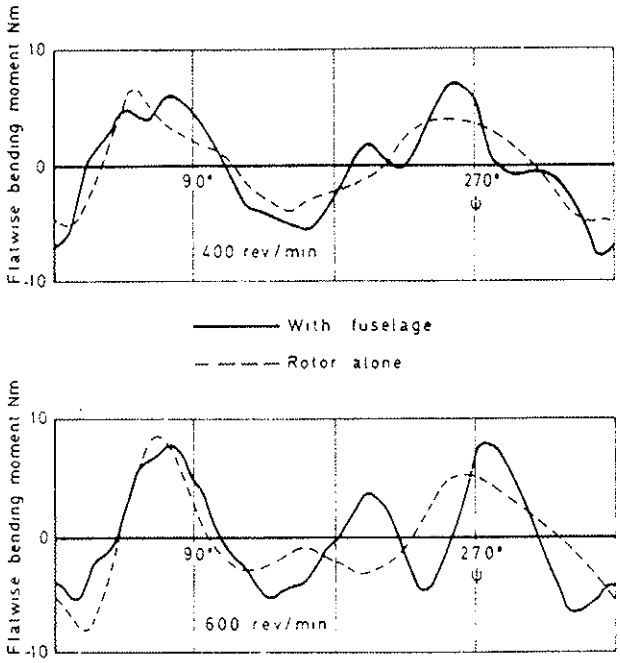

Fig 17 Measured variation of blade flatwise bending moment for model rotor at two rotor speeds for $\mu = 0.3$

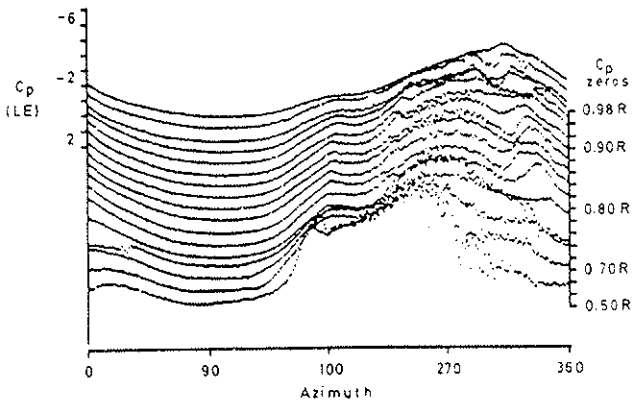

Fig 18 Measured variation of leading-edge pressures on a Puma blade in forward flight

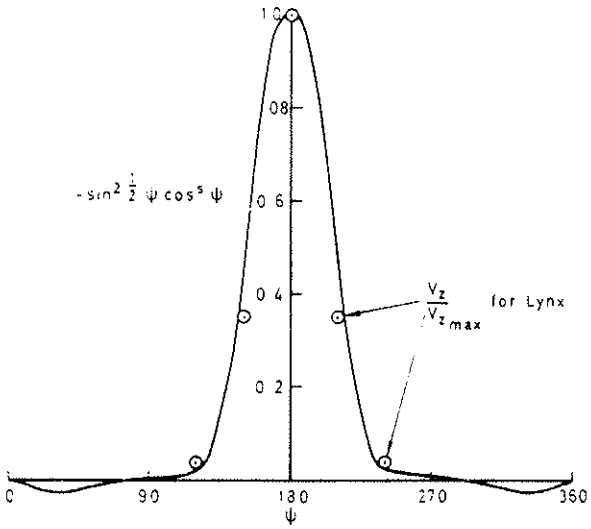

Fig 19 Tip vortex distortion function compared with azimuthal variation of fuselage upwash at 40% rotor radius for Lynx

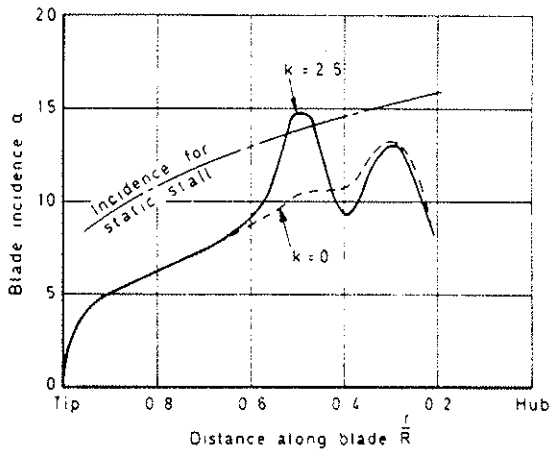

Fig 20 Predicted effect of vortex wake distortion on blade incidence at 180° azimuth for Lynx at 140 knots

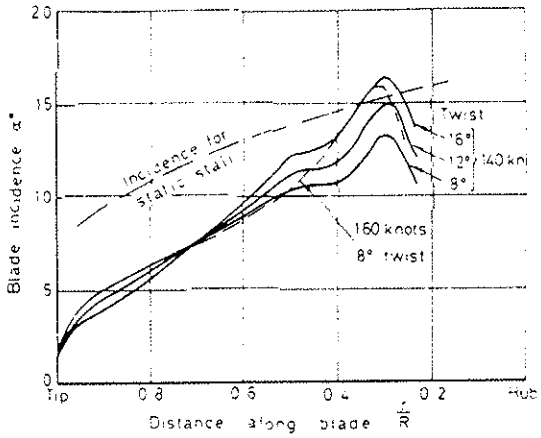

Fig 21 Predicted effect of increased forward speed and blade twist on blade incidence for Lynx rotor at 180° azimuth

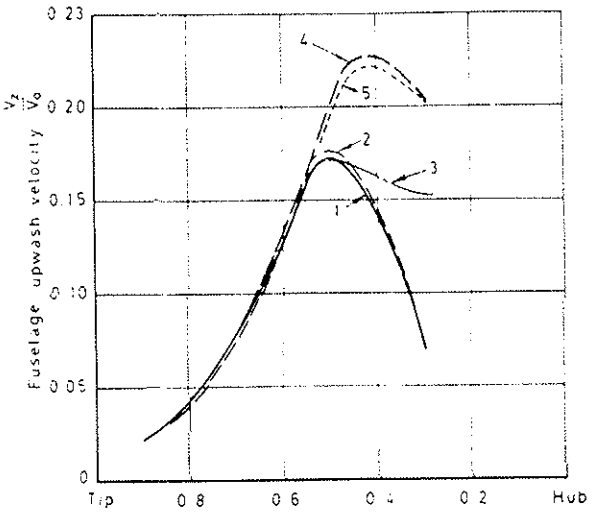

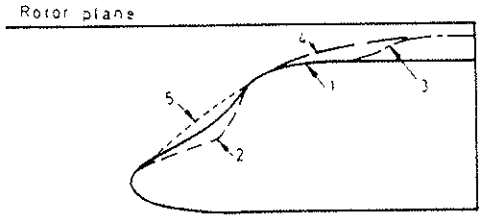

Fig 22 Predicted upwash in plane of rotor for various fuselage shapes at 180° azimuth

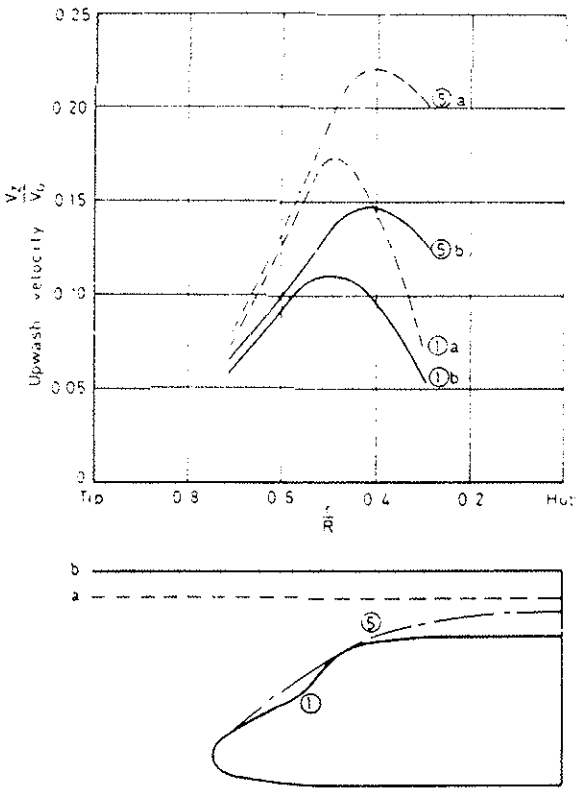

Fig 23 Predicted variation of fuselage upwash with height above fuselage at 180° azimuth for two fuselage shapes

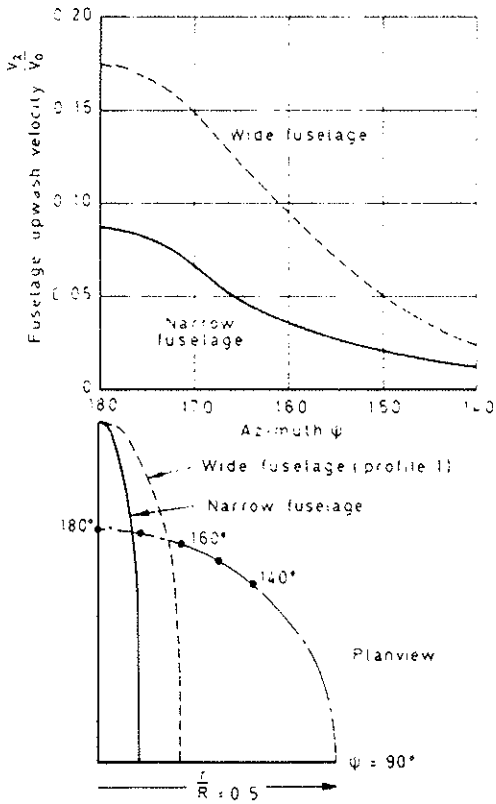

Fig 24 Effect of fuselage width on upwash velocity in plane of rotor at 50% radius

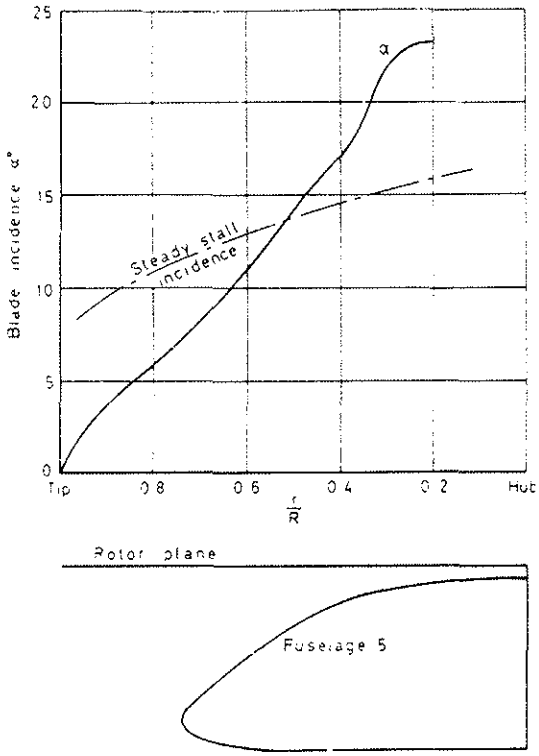

Fig 25 Predicted blade incidence at 180° azimuth for rotor of Lynx dimensions with 16° twist with fuselage configuration shown at 140 knots

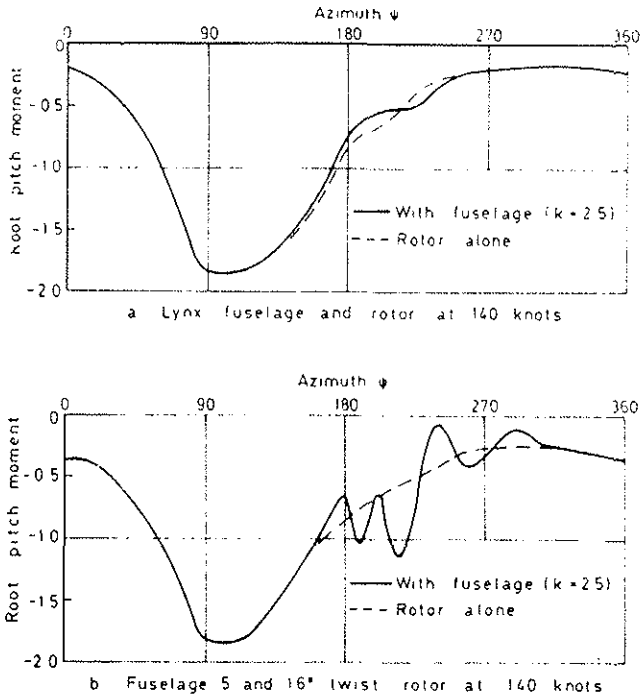

Fig 26a&b Calculated blade root pitching moment as a multiple of mean value for rotor alone, showing effect of blade stall at 180° azimuth for fuselage 5 and high twist blade